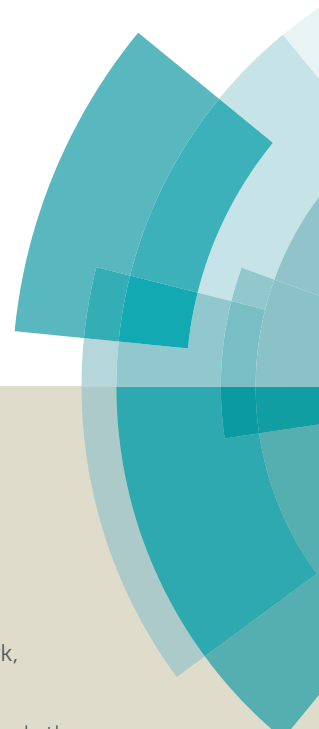
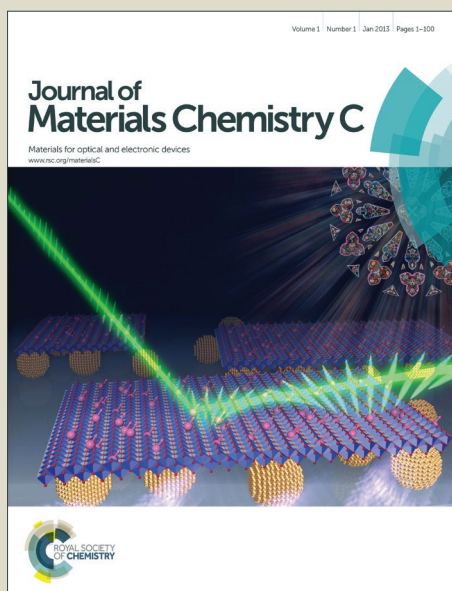


# Journal of Materials Chemistry C

Accepted Manuscript



This article can be cited before page numbers have been issued, to do this please use: J. Kim, J. B. Park, S. C. Yoon, I. H. Jung and D. Hwang, *J. Mater. Chem. C*, 2016, DOI: 10.1039/C5TC04449A.



This is an *Accepted Manuscript*, which has been through the Royal Society of Chemistry peer review process and has been accepted for publication.

*Accepted Manuscripts* are published online shortly after acceptance, before technical editing, formatting and proof reading. Using this free service, authors can make their results available to the community, in citable form, before we publish the edited article. We will replace this *Accepted Manuscript* with the edited and formatted *Advance Article* as soon as it is available.

You can find more information about *Accepted Manuscripts* in the [Information for Authors](#).

Please note that technical editing may introduce minor changes to the text and/or graphics, which may alter content. The journal's standard [Terms & Conditions](#) and the [Ethical guidelines](#) still apply. In no event shall the Royal Society of Chemistry be held responsible for any errors or omissions in this *Accepted Manuscript* or any consequences arising from the use of any information it contains.



## ARTICLE

## Enhanced and controllable open-circuit voltage using 2D-conjugated benzodithiophene (BDT) homopolymers by alkylthio substitution

Received 00th January 20xx,  
Accepted 00th January 20xx

DOI: 10.1039/x0xx00000x

www.rsc.org/

Ji-Hoon Kim,<sup>a</sup> Jong Baek Park,<sup>a</sup> Sung Cheol Yoon,<sup>b</sup> In Hwan Jung,<sup>b\*</sup> Do-Hoon Hwang<sup>a\*</sup>

In this study, we explore the effects of alkylthiophene (T) and alkylthiothiophene (T-S) substituents on the benzo[1,2-b;4,5-b']dithiophene (BDT) unit by comparing the BDTT homopolymer (PBDDT), BDTT-*alt*-BDTT-S copolymer (PBDDT-BDTT-S), and BDTT-S homopolymer (PBDDT-S) in terms of UV-visible absorption spectra, cyclic voltammetry (CV) results, computational calculations, and experimental results. The T-S substituent increased the hole mobility of the polymer and down-shifted the highest occupied molecular orbital (HOMO) energy level of the polymer, leading to slight red-shifting of the absorption spectrum. The organic photovoltaic (OPV) cells based on PBDDT-S as a donor and [6,6]-phenyl-C<sub>71</sub>-butyric acid methyl ester (PC<sub>71</sub>BM) as an acceptor demonstrated a high power conversion efficiency (PCE) of 7.05% under AM 1.5G illumination (100 mW cm<sup>-2</sup>). To the best of our knowledge, this PCE value is one of the highest values reported for homopolymer donor-based OPVs. Compared to the well-known P3HT homopolymer, which shows a similar absorption profile, PBDDT-S is a promising candidate for organic photodiodes.

### Introduction

Bulk heterojunction (BHJ) organic photovoltaic cells (OPVs), in which a blended film consisting of a conjugated polymer (the donor) and fullerene derivative (the acceptor) acts as the active layer, have attracted considerable attention in both academia and industry because of their low cost, light weight, easy fabrication, and potential for use in flexible devices.<sup>1–3</sup> Over the past few years, rapid progress has been made in this field, and power conversion efficiencies (PCEs) of 10% for single junction OPVs and 11% for tandem OPVs have been achieved.<sup>4–9</sup> Donor polymers consisting of electron donating (D) and accepting (A) units have been extensively investigated in order to achieve broader absorption spectra and deep highest occupied molecular orbital (HOMO) energy levels for producing highly efficient OPVs. However, D-A type copolymers require multiple synthesis steps to produce more than two different types of monomers.<sup>10–14</sup> On the other hand, the synthesis of homopolymers is highly attractive since they require only one D unit. Thus, full donor-type polymers such as poly(3-hexylthiophene) (P3HT) are potentially advantageous because they have simpler structures, shorter synthetic routes, and lower polymerization time-costs than D-A copolymer-based systems.<sup>15–18</sup> These D type polymers are usually wide bandgap analogs, which are highly important for use in the bottom cell of multi-junction devices. To overcome the current PCE limitations of tandem cells (~11.6%), the development of new electron donating homopolymers is required.<sup>8</sup>

Recently, *Kim and co-workers* showed a bright future with a BDT-based homopolymer, i.e., poly{4,8-bis(5-(2-ethylhexyl)thiophen-2-yl)benzo[1,2-b:4,5-b']dithiophene} (PBDDT), which exhibited a deep HOMO energy level. The OPV device fabricated using PBDDT had a PCE of 6.12%, benefitting from both high  $V_{OC}$  (0.93V) and  $J_{SC}$  (11.95 mA cm<sup>-2</sup>) values.<sup>20</sup> Furthermore, *Lee et al.* introduced dialkylthio side chains on BDT for tuning the optoelectronic properties of PBDDT derivatives and found that PBDDT derivatives with the dialkylthio side chain possessed a down-shifted HOMO energy level compared to that of PBDDT with a dialkoxy side chain.<sup>21</sup> Later, *Li et al.* attached an alkylthiothiophene side chain on the BDT unit for two-dimensional (2D)-conjugated polymers, and the HOMO energy levels of the BDT-based polymers were also effectively down-shifted so that a high  $V_{OC}$  was achieved in OPVs.<sup>22,23</sup>

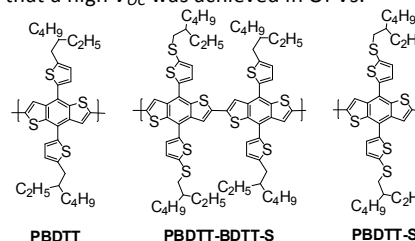


Fig. 1. Chemical structures of polymers in this research.

In this study, we designed and synthesized a series of BDT-based conjugated polymers by introducing different 2D-conjugated side chains of alkylthiophene (BDTT) or alkylthiothiophene (BDTT-S). Three polymers, poly{4,8-bis(5-(2-ethylhexyl)thiophen-2-yl)benzo[1,2-b:4,5-b']dithiophene} (PBDDT), poly{4,8-bis(5-(2-ethylhexyl)thiophen-2-yl)benzo[1,2-b:4,5-b']dithiophene-*alt*-4,8-bis(5-(2-ethylhexyl)thio)thiophen-2-yl)benzo[1,2-b:4,5-b']-dithiophene} (PBDDT-BDTT-S), and

<sup>a</sup>Department of Chemistry and Chemistry Institute for Functional Materials, Pusan National University, Busan 609-735, Republic of Korea

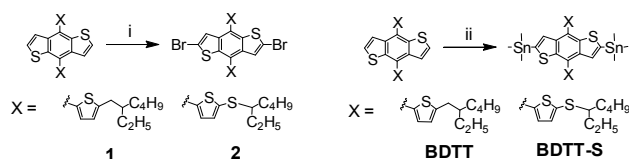
<sup>b</sup>Advanced Materials Division, Korea Research Institute of Chemical Technology (KRICT), Daejeon 305-600, Republic of Korea

\*Correspondence - dohoonhwang@pusan.ac.kr

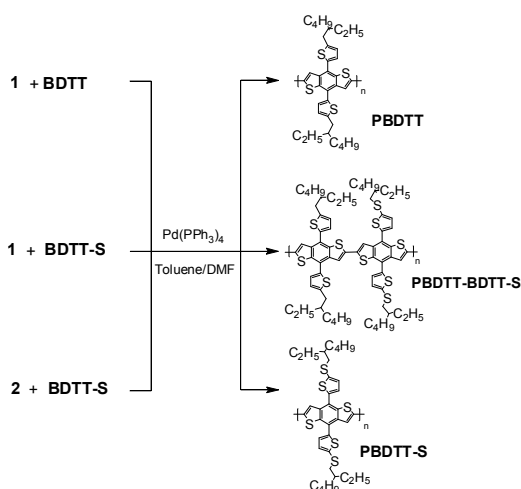
## ARTICLE

## Journal of Materials Chemistry C

poly[4,8-bis(5-((2-ethylhexyl)thio)thiophen-2-yl)benzo[1,2-b:4,5-b']-dithiophene] (PBDDT-S), were synthesized as shown in Fig. 1. Interestingly, the replacement of alkylthiophene with alkylthiothiophene significantly altered the optical, electrochemical, and morphological properties of the polymers. There are also stark differences in the characteristics of BHJ OPV devices prepared with PBDDT, PBDDT-BDDT-S, or PBDDT-S and PC<sub>71</sub>BM. Our device analyses suggest PBDDT-S-based BHJ OPVs exhibited notably improved charge separation and extraction, resulting in a promising PCE of 7.05%, which is the highest value reported for devices fabricated using full donor type polymers.



**Scheme 1.** Synthetic route and chemical structure of monomers. Reagents and conditions: (i) *n*-BuLi, CBr<sub>4</sub>, -78 °C, overnight; (ii) TMEDA, *n*-BuLi, trimethyltinchloride, -78 °C, overnight.



**Scheme 2.** Synthesis and chemical structure of the polymers; polymerization conditions: [Pd(PPh<sub>3</sub>)<sub>4</sub>], toluene/DMF (4:1), reflux, 16 h.

## Results and discussion

### Synthesis and Characterization of the Polymers

The synthetic routes and chemical structures of the monomers and polymers are outlined in Schemes 1 and 2, respectively. 4,8-Bis(5-(2-ethylhexyl)thiophen-2-yl)benzo[1,2-b:4,5-b']dithiophene and 4,8-bis(5-((2-ethylhexyl)thio)thiophen-2-yl)benzo[1,2-b:4,5-b']-dithiophene (1) were synthesized according to reported procedures.<sup>24–26</sup> PBDDT, PBDDT-BDDT-S, and PBDDT-S were subsequently prepared by Stille-coupling polymerization with dibromo BDDT or BDDT-S and dithiophene monomers using a Pd(PPh<sub>3</sub>)<sub>4</sub> catalyst. The crude copolymers were purified by successive washing with hot methanol, hexane, and acetone using a Soxhlet extractor. Both copolymers are soluble in common organic solvents, such as chloroform (CF), chlorobenzene (CB), and *o*-dichlorobenzene (*o*-DCB). The average molecular weights and

polydispersity indices (PDIs) of the polymers were determined using gel permeation chromatography (GPC) calibrated with polystyrene standards. The number average molecular weights (*M<sub>n</sub>*) of PBDDT, PBDDT-BDDT-S, and PBDDT-S were 20,000, 19,000, and 21,000 g/mol, respectively, with PDIs of 2.4, 2.2, and 2.2, respectively.

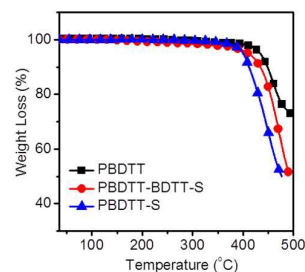


**Fig. 2.** Thermogravimetric analysis plots of the copolymers.

The thermal stability of the polymers was investigated by thermogravimetric analysis (TGA). PBDDT, PBDDT-BDDT-S, and PBDDT-S have good thermal stability with decomposition temperatures (5% weight loss) of 437, 417, and 401 °C, respectively (Fig. 2), indicating that the alkylthio hybrid electron-donating side chains decrease the thermal stability of the polymers slightly in comparison to the general alkyl side chain in PBDDT. Nevertheless, the thermal stabilities of PBDDT-BDDT-S and PBDDT-S are sufficient for application in OPVs. Table 1 summarizes the molecular weights and thermal properties of the synthesized copolymers.

**Table 1.** Average molecular weights and thermal properties of the synthesized polymers.

Polymer	<i>M<sub>n</sub></i> <sup>[a]</sup> (g/mol)	<i>M<sub>w</sub></i> <sup>[a]</sup> (g/mol)	<i>PDI</i> <sup>[a]</sup>	<i>T<sub>d</sub></i> <sup>[b]</sup> (°C)
PBDDT	20,000	48,000	2.4	436
PBDDT-BDDT-S	19,000	43,000	2.2	410
PBDDT-S	21,000	46,000	2.2	401

<sup>[a]</sup>*M<sub>n</sub>*, *M<sub>w</sub>*, and *PDI* of the polymers were determined by gel permeation chromatography using a polystyrene standard in CHCl<sub>3</sub>. <sup>[b]</sup>Temperature at which 5% weight loss was observed with a heating rate of 10 °C/min under N<sub>2</sub>.

### Optical and Electrochemical Properties

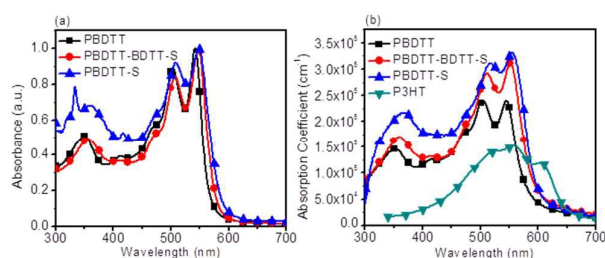
Figs. 3a and b show the absorption spectra of PBDDT, PBDDT-BDDT-S, and PBDDT-S in dilute CF solution and as thin films, respectively. The corresponding absorption data are listed in Table 2. The absorption spectra of the three polymer thin films each show three absorption peaks, including a distinct absorption peak at ~505 nm ascribed to the π-π\* transition between BDT units, and a peak at ~550 nm attributed to the vibronic peak. The absorption spectra in the solution states are similar to those of the thin film states, indicating that a certain degree of packing occurs in the solution state.<sup>27,28</sup> Interestingly, the absorption maxima and onset positions of the BDDT-S-based polymers (PBDDT-BDDT-S and PBDDT-S) are red-shifted by 5 and 10 nm, respectively, in comparison to that of PBDDT due to extension of the effective π-conjugation length by introduction of the alkylthio group. The optical bandgaps of PBDDT, PBDDT-BDDT-S, and PBDDT-S were calculated from the absorption edge of the thin films to be 2.12, 2.09, and 2.06 eV, respectively. Compared to the absorption spectrum of P3HT (*E<sub>g</sub>* ~1.9 eV, Fig.

**Table 2.** Optical and electrochemical properties of synthesized polymers.

Polymers	$\lambda_{\max, \text{abs}}$ (nm)	$\lambda_{\max}$ (nm)	$\lambda_{\text{edge}}$ (nm)	Optical $E_g^{\text{opt}}$ (eV) <sup>[b]</sup>	HOMO <sup>[c]</sup> (eV)	LUMO <sup>[d]</sup> (eV)
	Solution	Film <sup>[a]</sup>	Film <sup>[a]</sup>			
PBDTT	503, 542	504, 545	585	2.12	-5.40	-3.28
PBDTT-BDTT-S	506, 548	510, 550	593	2.09	-5.54	-3.45
PBDTT-S	508, 550	517, 554	598	2.06	-5.58	-3.52

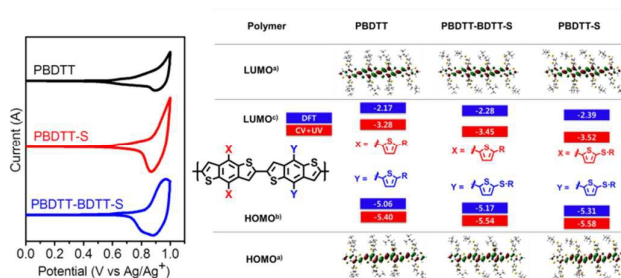
<sup>[a]</sup> Polymer film on a quartz plate formed by spin-casting from chloroform solution at 1500 rpm for 30 s. <sup>[b]</sup> Calculated from the UV-visible absorption edge of the polymer films,  $E_g = 1240/\lambda_{\text{edge}}$ . <sup>[c]</sup> HOMO =  $-(E_{\text{ox}}^{\text{onset}} + 4.708)$  (eV), <sup>[d]</sup> LUMO =  $E_g^{\text{opt}} + \text{HOMO}$  (eV).

**3b**), the absorbance of the synthesized polymers is much higher in the short wavelength region from 300 to 450 nm, making these materials suitable for high-energy photon harvesting. Interestingly, the absorption coefficients of PBDTT, PBDTT-BDTT-S, and PBDTT-S are  $2.4 \times 10^5$ ,  $3.0 \times 10^5$ , and  $3.3 \times 10^5$   $\text{cm}^{-1}$ , respectively, which are higher than that of P3HT ( $1.5 \times 10^5$   $\text{cm}^{-1}$ ), indicating that the three polymers can absorb sunlight more efficiently than the P3HT film with the same thickness. Moreover, the measured absorption coefficients of the alkylthio-substituted thiophene BDT containing polymers (PBDTT-BDTT-S and PBDTT-S) are higher than that of PBDTT.

**Fig. 3.** Optical properties: UV-visible absorption spectra of polymers in (a) CF solution and (b) film state on quartz.

To determine the HOMO and LUMO energy levels of the resulting polymers, the electrochemical characteristics of the polymer films on a Pt electrode were investigated by cyclic voltammetry (CV) with 0.1 M tetrabutylammonium tetrafluoroborate (TBABF<sub>4</sub>) as the supporting electrolyte and Ag/AgNO<sub>3</sub> as the reference electrode (**Fig. 4a**). To obtain the oxidation potentials, the reference electrode was calibrated using ferrocene/ferrocenium (Fc/Fc<sup>+</sup>), which has an absolute energy level of -4.80 eV with respect to the vacuum level; the potential of this external standard under the same conditions was 0.091 eV. Accordingly, the HOMO values ( $E_{\text{HOMO}}$ ) were calculated using the following equation:  $E_{\text{HOMO}} = -(E_{\text{ox}}^{\text{onset}} + 4.708)$  eV, where  $E_{\text{ox}}^{\text{onset}}$  is the onset oxidation potential versus Ag/Ag<sup>+</sup>. The onset oxidation potentials ( $E_{\text{ox}}$ ) of PBDTT, PBDTT-BDTT-S, and PBDTT-S are 0.692, 0.832, and 0.872, respectively, corresponding to HOMO energy levels of -5.40, -5.54, and -5.58 eV, respectively.

The HOMO energy levels of PBDTT-BDTT-S and PBDTT-S are lower than that of PBDTT because the alkylthio group has a  $\pi$ -accepting property when it connects with unsaturated aromatic rings such as the thiophene.<sup>29,30</sup> Meanwhile, the LUMO levels of the polymers were determined from the HOMO levels obtained from the CV measurements and the  $E_g^{\text{opt}}$  values obtained from the UV-visible absorption edges.

**Fig. 4.** (Left) CV curves of polymers. (Right) (a) Energy-minimized structure (B3LYP/6-31G\*) of the HOMO (bottom) and LUMO (top) of the tetramer model compounds. (b) The HOMO energy levels were measured by cyclic voltammetry as thin films. (c) The LUMO energy was estimated by adding the absorption onset to the HOMO.

The LUMO energy levels of the polymers are within a suitable range (-3.38 to -3.46 eV) and are higher-lying than that of PC<sub>71</sub>BM (ca. -4.30 eV); thus, efficient charge transfer (exciton dissociation) can be expected in the corresponding devices.<sup>31</sup> The HOMO and LUMO energy levels of the polymers are illustrated in **Fig. 4b**. The UV-visible absorption properties,  $E_g^{\text{opt}}$  values, and HOMO/LUMO energy levels of the polymers are summarized in **Table 2**.

### Theoretical Calculations

Density functional theory (DFT) calculations were performed using B3LYP functional and 6-31G(d) basis sets to better understand the electronic structures of the polymers and, in particular, the effects of introducing the side chains onto the BDT units. Calculations were performed on tetramers as simplified models. The frontier molecular orbitals and optimized molecular geometries of the three polymers are illustrated in **Fig. 4**. The alkyl chains are further simplified by replacing the 2-ethylhexyl group of the BDTT and BDTT-S unit with methylpropyl groups. Calculations were carried out using the Gaussian 09 program package.<sup>32</sup> According to these model calculations, both the HOMO and LUMO energy levels could be lowered by replacing alkylthiophene with alkylthiothiophene. The trend of the HOMO and LUMO energy levels reflects the experimental results: the HOMO energy level increases in the order of PBDTT < PBDTT-BDTT-S < PBDTT-S. Therefore, all of the above results indicate that the polymers will exhibit different  $V_{\text{OC}}$  values when used in OPV devices and the  $V_{\text{OC}}$  could be varied by controlling the amount of the two components (PBDTT and PBDTT-S).<sup>33</sup>

### Photovoltaic Performance and Hole mobility

To explore the potential of the three polymers in OPVs, BHJ type OPVs were fabricated with a conventional device configuration (indium tin oxide (ITO)/PEDOT:PSS/polymer:PC<sub>71</sub>BM/Ca/Al) and

**Table 3.** Comparison photovoltaic properties of OPVs based on polymer:PC<sub>71</sub>BM with different weight ratios, measured under AM 1.5 G illumination, 100 mW cm<sup>-2</sup>.

Polymer	Ratio	$V_{OC}^{[a]}$ [V]	$J_{SC}^{[a]}$ [mA cm <sup>-2</sup> ]	$FF^{[a]}$ [%]	$PCE^{[a]}$ [%] Best (Ave)	$\mu_h^{[c]}$ [cm <sup>2</sup> V <sup>-1</sup> s <sup>-1</sup> ]
PBDTT	1 : 1	0.92	11.59 [11.00] <sup>[b]</sup>	42	4.45 (4.21)	$1.87 \times 10^{-5}$
	1 : 2	0.89	9.91 [9.41] <sup>[b]</sup>	47	4.09 (3.98)	
	1 : 3	0.89	7.59 [7.20] <sup>[b]</sup>	53	3.49 (3.40)	
PBDTT-BDTT-S	1 : 1	0.96	13.15 [12.47] <sup>[b]</sup>	49	6.14 (6.08)	$4.73 \times 10^{-4}$
	1 : 2	0.92	12.74 [12.04] <sup>[b]</sup>	52	6.07 (5.96)	
	1 : 3	0.90	10.50 [10.00] <sup>[b]</sup>	53	5.03 (4.88)	
PBDTT-S	1 : 1	0.99	13.92 [13.25] <sup>[b]</sup>	51	7.05 (6.98)	$9.33 \times 10^{-4}$
	1 : 2	0.93	12.18 [11.54] <sup>[b]</sup>	55	6.25 (6.10)	
	1 : 3	0.92	11.88 [11.26] <sup>[b]</sup>	56	6.07 (5.99)	

<sup>[a]</sup>Photovoltaic properties of copolymers/PC<sub>71</sub>BM-based devices spin-coated from a dichlorobenzene solution for polymers. <sup>[b]</sup>Calculated  $J_{SC}$  from the EQE spectra. <sup>[c]</sup>The SCLC devices with structure of ITO/PEDOT:PSS (30 nm)/polymer:PC<sub>71</sub>BM (1:1)/Au.

their performances were measured using an AM 1.5G solar simulator. PC<sub>71</sub>BM was chosen as the electron acceptor instead of PC<sub>61</sub>BM because it absorbs more light in the visible range. We fabricated photovoltaic devices using various donor to acceptor weight ratios (1.0:1.0, 1.0:2.0, and 1.0:3.0) to optimize the PCEs. The best device performance was obtained using 10 mg/mL of the polymer in *o*-DCB for spin-coating, with a polymer:PC<sub>71</sub>BM ratio of 1.0:1.0 (w/w). The thicknesses of the PBDTT, PBDTT-BDTT-S, and PBDTT-S films with PC<sub>71</sub>BM were all similar (~100 nm), as measured using an alpha-step profiler. The  $V_{OC}$ ,  $J_{SC}$ ,  $FF$ , and PCE values of the fabricated devices are summarized in Table 3.

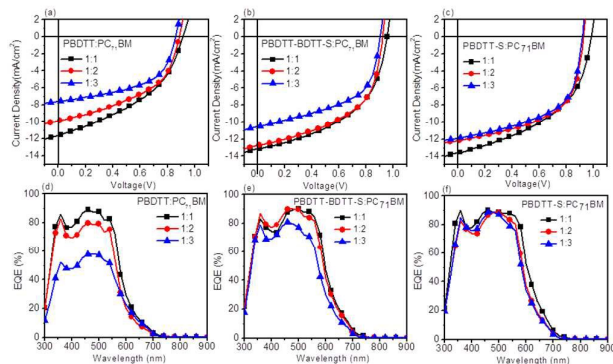


**Fig. 5.** Current density-voltage ( $J$ - $V$ ) curves of OPVs with different blend ratios. (a) PBDTT:PC<sub>71</sub>BM, (b) PBDTT-BDTT-S:PC<sub>71</sub>BM, and (c) PBDTT-S:PC<sub>71</sub>BM under AM 1.5G illumination, 100 mW cm<sup>-2</sup>. External quantum efficiency (EQE) curves of OPVs at different blend ratios based on (d) PBDTT:PC<sub>71</sub>BM, (e) PBDTT-BDTT-S:PC<sub>71</sub>BM, and (f) PBDTT-S:PC<sub>71</sub>BM.

Fig. 5 shows the current density-voltage ( $J$ - $V$ ) curves of the OPVs and external quantum efficiencies (EQEs) of the devices based on the polymer:PC<sub>71</sub>BM blends under AM 1.5G illumination (100 mW/cm<sup>2</sup>). The PCEs of the devices increase in the order of PBDTT (4.45%) < PBDTT-BDTT-S (6.14%) < PBDTT-S (7.05%), which indicates a linear dependence between the device performance and the number of BDTT-S units in the polymer backbone. Similarly, the  $V_{OC}$  values of each optimized device increase gradually from 0.92 to 0.99 V, depending on the number of BDTT-S units in the polymer backbone.  $V_{OC}$  is mainly determined by the difference between the HOMO energy level of the donor polymer and the LUMO energy level of the acceptor (PC<sub>71</sub>BM). Thus, the down-shifted HOMO energy levels result in the higher  $V_{OC}$  values of the devices: the

higher  $V_{OC}$  of the PBDTT-S polymer is a result of the deeper HOMO energy level (-5.58 eV) of PBDTT-S, compared to PBDTT (-5.40 eV) and PBDTT-BDTT-S (-5.54 eV).<sup>34</sup>

Interestingly, the  $J_{SC}$  values of the devices fabricated using the three polymers are significantly different. The measured  $J_{SC}$  values of the devices fabricated using PBDTT, PBDTT-BDTT-S, and PBDTT-S are 11.59, 13.15, and 13.92 mA cm<sup>-2</sup>, respectively. The  $J_{SC}$  of OPVs is affected by many factors, including the absorption strength of the active layer, the charge carrier mobility, and film morphology. We believe that the high  $J_{SC}$  values of the PBDTT-BDTT-S and PBDTT-S devices could potentially be a result of the enhanced light absorption properties.<sup>12,13,34</sup>

In order to evaluate the hole mobility ( $\mu_h$ ) of the resulting polymers, hole-only devices with a configuration of ITO/PEDOT:PSS (30 nm)/polymer:PC<sub>71</sub>BM (1.0:1.0 w/w) (blend state)/Au were fabricated and the hole mobilities were obtained using the space-charge-limited current (SCLC) model (Fig. 6). The extracted  $\mu_h$  values are listed in Table 3. At higher voltages (in the SCLC region), the  $J$ - $V$  characteristics can be fitted with the Mott-Gurney equation:

$$J_{SCLC} = (9/8) \epsilon_r \epsilon_0 \mu (V^2/L^3)$$

where  $\epsilon_0$  is the free-space permittivity ( $8.85 \times 10^{-14}$  C V<sup>-1</sup> cm<sup>-1</sup>),  $\epsilon_r$  is the relative dielectric constant (3.2),  $V = V_{appl} - V_{bi}$  ( $V_{appl}$  is the applied potential and  $V_{bi}$  is the built-in voltage that results from the difference in the work function of the anode and cathode), and  $L$  is the film thickness. The measured hole mobilities of the PBDTT:PC<sub>71</sub>BM (1.0:1.0, w/w), PBDTT-BDTT-S:PC<sub>71</sub>BM (1.0:1.0, w/w), and PBDTT-S:PC<sub>71</sub>BM (1.0:1.0, w/w) blends are  $1.87 \times 10^{-5}$ ,  $4.73 \times 10^{-4}$ , and  $9.33 \times 10^{-4}$  cm<sup>2</sup> V<sup>-1</sup> s<sup>-1</sup>, respectively.

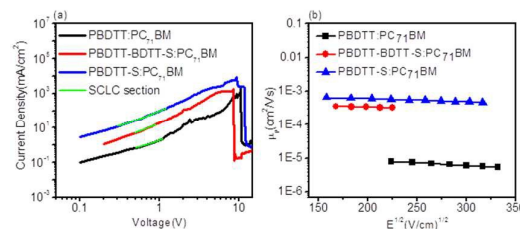


**Fig. 6.** (a)  $J$ - $V$  characteristics of the hole-only devices and (b) field-dependent hole mobilities of polymer:PC<sub>71</sub>BM (1.0:1.0, w/w) blend films calculated from the hole-only devices by fitting the  $J$ - $V$  curves in the SCLC regime.

Considering that PBDTT-S shows higher hole mobility and superior absorption than PBDTT and PBDTT-BDTT-S, the high  $J_{SC}$  of the PBDTT-S device appears to result primarily from the improved

optical absorption coefficients and high hole mobility. It should be noted that incorporation of the alkylthio-thiophene side chain into the BDT units significantly increases the absorption coefficient and hole mobility, thereby enhancing the  $J_{SC}$  and PCE values of the PBDTT-S solar cell devices. It is also noteworthy that the accuracy of the  $J_{SC}$  value was further confirmed by EQE measurements under illumination of monochromatic light. The EQE spectra are shown in Fig. 5. Compared to the absorption spectra of pristine polymers, the substantially broadened EQE responses in the visible region can be attributed to both the intrinsic absorptions of the polymers and PC<sub>71</sub>BM. The calculated current densities from the EQE measurements are 11.00, 12.47, and 13.25 mA cm<sup>-2</sup> for PBDTT:PC<sub>71</sub>BM (1.0:1.0, w/w), PBDTT-BDTT-S:PC<sub>71</sub>BM (1.0:1.0, w/w), and PBDTT-S:PC<sub>71</sub>BM (1.0:1.0, w/w), respectively. The  $J_{SC}$  values calculated from integration of the EQE spectra are within 3–5% error, which conform well to those obtained from the  $J$ - $V$  measurements, supporting the reliability of the photovoltaic measurements. PBDTT-S:PC<sub>71</sub>BM devices showing EQE over 80% in the visible area are also excellent candidates for organic photodiode image sensors. We calculated the sensitivity ( $S(\lambda)$ ) of photodiodes based on PBDTT-S at the 0 voltages to evaluate this possibility. The sensitivity ( $S(\lambda)$ ) graph for the PBDTT-S:PC<sub>71</sub>BM films is shown in Fig. 7. In the range of 360–580 nm, the PBDTT-S:PC<sub>71</sub>BM device follows the ideal sensitivity line, which shows its great potential as a photodiode material at the corresponding wavelength area.

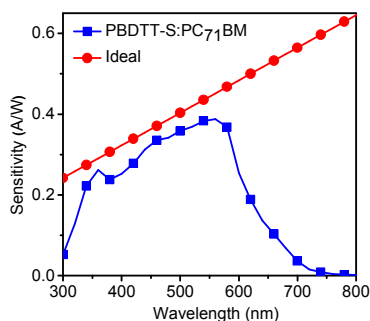


Fig. 7. Sensitivity of PBDTT-S:PC<sub>71</sub>BM (1:1) based photodiodes depending on wavelength.

The surface and bulk morphologies of the polymer:PC<sub>71</sub>BM blend films were studied by atomic force microscopy (AFM) and transmission electron microscopy (TEM), respectively. As shown in Fig. 8d–f, all of the blend films exhibit uniform and bi-continuous networks, indicating good miscibility between the polymer donor and PC<sub>71</sub>BM. The interpenetrating network between the polymers and PC<sub>71</sub>BM provides a large interface area for efficient charge separation and transportation to achieve high  $J_{SC}$  and  $FF$  values in OPVs. The mean square surface roughness ( $R_q$ ) of the PBDTT:PC<sub>71</sub>BM, PBDTT-BDTT-S:PC<sub>71</sub>BM, and PBDTT-S:PC<sub>71</sub>BM blend films are 4.04, 2.84, and 1.66 nm, respectively. In addition, as clearly observed in the TEM images, both of the PBDTT:PC<sub>71</sub>BM and PBDTT-BDTT-S:PC<sub>71</sub>BM films show uniform and relatively small domains with a length scale of a few tens of nanometers. For the PBDTT-S:PC<sub>71</sub>BM film, nano fibril domains can be clearly observed.

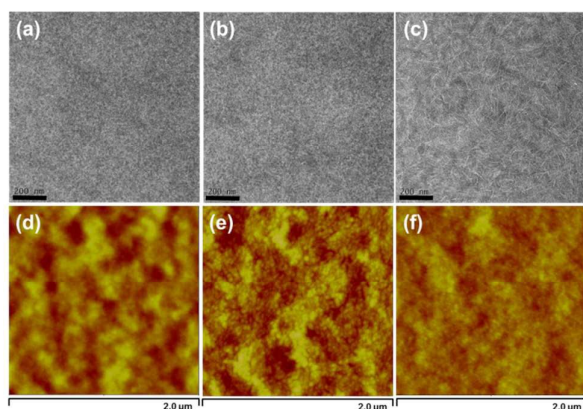


Fig. 8. TEM and AFM images of polymer:PC<sub>71</sub>BM blend films (1.0:1.0 w/w) cast from *o*-dichlorobenzene: (a, d) PBDTT:PC<sub>71</sub>BM (1.0:1.0 w/w), (b, e) PBDTT-BDTT-S:PC<sub>71</sub>BM (1.0:1.0 w/w), and (c, f) PBDTT-S:PC<sub>71</sub>BM (1.0:1.0 w/w).

It should be noted that we do not rule out other factors that could be responsible for the superior performance of the PBDTT-S:PC<sub>71</sub>BM device since  $J_{SC}$  is known to be affected by other factors, such as the absorption strength of the active layer and charge-carrier mobility. The attributes of the wider absorption spectrum, stronger shoulder peak, and higher hole mobility of PBDTT-S are likely to have contributed to the higher  $J_{SC}$  values. Further studies are underway in order to clarify the contributions of each factor.

## Conclusions

In conclusion, we have successfully synthesized the BDTT homopolymer (PBDTT), BDTT-*alt*-BDTT-S copolymer (PBDTT-BDTT-S), and BDTT-S homopolymer (PBDTT-S) by Pd-catalyzed Stille cross-coupling polymerization for applications in OPVs. The polymers containing alkylthio side chains showed down-shifted HOMO energy levels and exhibited higher absorption coefficients than P3HT or the corresponding PBDTT. The BHJ OPVs based on PBDTT-S as a donor and PC<sub>71</sub>BM as an acceptor demonstrated a high  $V_{OC}$  of 0.98 V, leading to a high PCE of 7.05%, under AM 1.5G illumination (100 mWcm<sup>-2</sup>). Therefore, PBDTT-S has great potential for use as a novel polymer donor to replace P3HT as the wide band gap polymer in tandem solar cells and ternary blend solar cells. In addition, we demonstrated that the optimized performance of the PBDTT-S:PC<sub>71</sub>BM device was obtained without any solvent additive or thermal treatment, which makes PBDTT-S a promising candidate as a polymer donor for flexible, large area OPVs.

## Experimental

### Materials

All the starting organic compounds were purchased from Aldrich, Alfa Aesar, or TCI Korea, and used without further purification. Tetrakis(triphenylphosphine)palladium(0) (Pd(PPh<sub>3</sub>)<sub>4</sub>) was purchased from Strem. PC<sub>71</sub>BM was purchased from EM-index. The solvents were dried and purified by fractional distillation over sodium/benzophenone and handled in a moisture-free atmosphere. Column chromatography was performed using silica gel (Merck, Kieselgel 60 63-200 MYM SC). 4,8-Bis(5-(2-ethylhexyl)thiophen-2-

## ARTICLE

## Journal of Materials Chemistry C

yl)benzo[1,2-b:4,5-b']-dithiophene and 4,8-bis(5-((2-ethylhexyl)thio)thiophen-2-yl)benzo[1,2-b:4,5-b']-dithiophene were synthesized according to previously reported procedures.<sup>24–26</sup>

## Measurements

<sup>1</sup>H and <sup>13</sup>C NMR spectra were recorded using a Varian Mercury Plus 300 MHz spectrometer and the chemical shifts were recorded in units of ppm with chloroform as the internal standard. Elemental analysis was carried out using a Vario Micro Cube at the Korea Basic Science Institute (Busan, Korea). Absorption spectra were measured using a JASCO JP/V-570 model. The molecular weights of the polymers were determined by gel permeation chromatography (GPC) with polystyrene standards for calibration, using a Waters high-pressure GPC assembly (model M590). Thermal analyses were carried out on a Mettler Toledo TGA/SDTA 851<sup>e</sup> under an N<sub>2</sub> atmosphere with a heating and cooling rate of 10 °C/min. Cyclic voltammetry (CV) was performed on a CH Instruments Electrochemical Analyzer. The CV measurements were carried out using acetonitrile containing 0.1 M tetrabutylammonium tetrafluoroborate (TBABF<sub>4</sub>) as the supporting electrolyte, and Ag/AgNO<sub>3</sub>, Pt wire, and Pt as the reference, counter, and working electrodes, respectively.

## Fabrication of Photovoltaic Devices

The devices were fabricated with the structure ITO/PEDOT:PSS/polymer:PC<sub>71</sub>BM/Ca/Al. The procedure for cleaning the ITO surface included sonication and rinsing in distilled H<sub>2</sub>O, methanol, and acetone. The hole-transporting PEDOT:PSS layer (45 nm) was spin-coated onto each ITO anode from a solution purchased from Heraeus (Clevios<sup>TM</sup> P VP AI4083). Each polymer:PC<sub>71</sub>BM solution was then spin-coated onto the PEDOT:PSS layer. The polymer solution for spin-coating was prepared by dissolving the polymer (10 mg mL<sup>-1</sup>) in *o*-DCB. Ca and Al contacts were formed sequentially by vacuum deposition at a pressure of < 3 × 10<sup>-6</sup> Torr, providing an active area of 0.09 cm<sup>2</sup>.

## Measurement of OPV Devices

The thickness of the active layer was measured using a KLA Tencor Alpha-step IQ surface profilometer with an accuracy of ±1 nm. The *J*-*V* characteristics of the polymer photovoltaic cells were determined by illuminating the cells with simulated solar light (AM 1.5G) at an intensity of 100 mW/cm<sup>2</sup> using an Oriel 1000 W solar simulator. Electronic data were recorded using a Keithley 236 source-measure unit. All the characterization measurements were carried out under ambient conditions. The illumination intensity was calibrated using a standard Si photodiode detector from PV Measurements Inc., which was calibrated at the National Renewable Energy Laboratory (NREL). The EQE was measured as a function of wavelength in the range of 300–1100 nm using a Xenon Short Arc Lamp as the light source (McScience K3100 EQX). The light source was calibrated using a Si reference photodiode. The measurements were carried out after masking all but the active cell area of the fabricated device and the measurements were conducted under ambient conditions.

## Fabrication and Measurement of Hole-only Devices

The hole mobility of the active layer was determined by applying the space charge limited current (SCLC) model to the *J*-*V* measurement data. Hole-only devices containing the polymers

were fabricated on pre-patterned ITO substrates. After cleaning the ITO with an aqueous detergent, deionized water, acetone, and 2-propanol, the ITO was treated with UV-ozone for 15 min. A PEDOT:PSS (Clevios P VP AI4083) layer with a thickness of 30 nm was spin-coated on the substrate from an aqueous dispersion phase. The coated substrate was then baked at 120 °C for 60 min. Subsequently, a solution of the copolymer in *o*-DCB was spin-cast on the PEDOT:PSS layer to form a layer with a thickness of ~100 nm, and the samples were dried for 6 h at room temperature under vacuum. Finally, 10 nm of MoO<sub>3</sub> and 100 nm of Ag were thermally evaporated as the anode in vacuo at a base pressure of 3 × 10<sup>-6</sup> Torr, which completed the device fabrication. The SCLC method was employed to measure the hole-only mobility of the polymer/PC<sub>71</sub>BM blend using a device with an ITO/PEDOT:PSS/polymer:PC<sub>71</sub>BM/MoO<sub>3</sub>/Ag structure. The hole mobilities were calculated using the following equation:

$$J_{SCLC} = (9/8)\epsilon_r \epsilon_0 \mu (V^2/L^3)$$

In the above equation, *J* is the current density,  $\epsilon_r$  is the dielectric constant of the polymers,  $\epsilon_0$  is the permittivity of vacuum,  $\mu$  is the hole mobility, *L* is the thickness of the blend films, and  $V = V_{appl} - V_{bi}$  where  $V_{appl}$  and  $V_{bi}$  are the applied potential and built-in voltage, which results from the difference in the work functions of the anode and cathode, respectively.

## Synthesis of the Monomers and Polymers

**Synthesis of 2,6-dibromo-4,8-bis(5-(2-ethylhexyl)thiophen-2-yl)benzo[1,2-b:4,5-b']-dithiophene (1):** Under a N<sub>2</sub> atmosphere, 4,8-bis(5-(2-ethylhexyl)thiophen-2-yl)benzo[1,2-b:4,5-b']-dithiophene (2.00 g, 3.45 mmol) in dry THF (100 mL) was cooled to -78 °C followed by the dropwise addition of *n*-butyllithium (3.45 mL, 8.63 mmol, 2.5 M in hexane). The reaction mixture was stirred at -78 °C for 1 h and then warmed to room temperature. The solution was then cooled to -78 °C again before tetrabromomethane (2.86 g, 8.63 mmol) in THF (10 mL) was added. The mixture was slowly brought to room temperature and stirred overnight. Water was added to the reaction mixture and the aqueous phase was extracted with ethyl acetate three times. The organic layer was separated, dried over anhydrous MgSO<sub>4</sub>, and filtered; the resulting solution was then concentrated by evaporation. The desired pure compound was obtained as a yellow solid (2.25 g, 82% yield) after recrystallizing the yellow product in methylene chloride and methanol. <sup>1</sup>H NMR (300 MHz, CDCl<sub>3</sub>, ppm): δ 7.58 (s, 2H), 7.20 (d, 2H), 6.87 (d, 2H), 2.85 (d, 4H), 1.72 (m, 4H), 1.51–1.23 (m, 18H), 0.94 (m, 12H). <sup>13</sup>C NMR (75 MHz, CDCl<sub>3</sub>, ppm): δ 145.3, 138.0, 135.1, 133.3, 131.2, 128.4, 125.5, 123.7, 111.2, 45.0, 38.3, 35.7, 30.2, 26.4, 22.7, 15.6, 13.8.

**Synthesis of 2,6-dibromo-4,8-bis(5-((2-ethylhexyl)thio)thiophen-2-yl)benzo[1,2-b:4,5-b']-dithiophene (2):** Under a N<sub>2</sub> atmosphere, 4,8-bis(5-((2-ethylhexyl)thio)thiophen-2-yl)benzo[1,2-b:4,5-b']-dithiophene (2.00 g, 3.25 mmol) in dry THF (100 mL) was cooled to -78 °C followed by the dropwise addition of *n*-butyllithium (3.25 mL, 8.13 mmol, 2.5 M in hexane). The reaction mixture was stirred at -78 °C for 1 h and then warmed to room temperature. The solution was then cooled to -78 °C again before tetrabromomethane (2.69 g, 8.63 mmol) in THF (10 mL) was added. The mixture was slowly brought to room temperature and stirred overnight. Water was added to the reaction mixture and the aqueous phase was extracted with ethyl acetate three times. The organic layer was

separated, dried over anhydrous  $\text{MgSO}_4$ , and filtered; the resulting solution was then concentrated by evaporation. The desired pure compound was obtained as a yellow solid (2.12 g, 62% yield) after recrystallizing the yellow product in methylene chloride and methanol.  $^1\text{H}$  NMR (300 MHz,  $\text{CDCl}_3$ , ppm):  $\delta$  7.61 (s, 2H), 7.33 (d, 2H), 6.92 (d, 2H), 2.96 (d, 4H), 1.81 (m, 4H), 1.62–1.32 (m, 18H), 0.92 (m, 12H).  $^{13}\text{C}$  NMR (75 MHz,  $\text{CDCl}_3$ , ppm):  $\delta$  146.1, 140.3, 137.5, 136.4, 133.7, 130.0, 127.5, 124.8, 114.3, 46.2, 40.1, 36.3, 33.5, 28.2, 26.1, 16.2, 14.0.

**Synthesis of 2,6-bis(trimethyltin)4,8-bis(5-((2-ethylhexyl)thio)thiophen-2-yl)benzo[1,2-b:4,5-b']-dithiophene (BDTT):** 2,6-Bis(trimethyltin)-4,8-bis(5-(2-ethylhexyl)thiophen-2-yl)benzo[1,2-b:4,5-b']dithiophene (BDTT) was synthesized according to the methods described in previous reports.<sup>26</sup>

**Synthesis of 2,6-bis(trimethyltin)4,8-bis(5-((2-ethylhexyl)thio)thiophen-2-yl)benzo[1,2-b:4,5-b']-dithiophene (BDTT-S):** 2,6-Bis(trimethyltin)4,8-bis(5-((2-ethylhexyl)thio)thiophen-2-yl)benzo[1,2-b:4,5-b']-dithiophene (BDTT-S) was synthesized according to the methods described in previous reports.<sup>22</sup>

#### General Polymerization Procedure

The three polymers were synthesized by Stille coupling polymerization, as shown in **Scheme 2**. Tetrakis(triphenylphosphine)palladium in 4 mL anhydrous toluene and 1 mL DMF was stirred at 110 °C overnight, and then an excess of 2-bromothiophene and tripropyl(thiophen-2-yl)stannane, the end-capper, dissolved in 1 mL of anhydrous toluene was added and stirred for 12 h. The reaction mixture was cooled to ~50 °C and 200 mL of methanol was added slowly with vigorous stirring. The polymer fibers were collected by filtration and were re-precipitated from methanol and acetone. The polymers were then purified further by washing for 1 day in a Soxhlet apparatus with acetone to remove oligomers and catalyst residues. Column chromatography with chloroform was then performed. Re-precipitation in chloroform/methanol was repeated several times. The resulting polymers were soluble in common organic solvents.

**Poly{4,8-bis((2-ethylhexyl)thiophen-2-yl)-benzo[1,2-b:4,5-b']dithiophene} (PBDTT):** 2,6-Bis(trimethyltin)4,8-bis(5-((2-ethylhexyl)thiophen-2-yl)benzo[1,2-b:4,5-b']-dithiophene (BDTT) (300 mg, 0.44 mmol) was mixed with 2,6-dibromo-4,8-bis(5-(2-ethylhexyl)thiophen-2-yl)benzo[1,2-b:4,5-b']-dithiophene (1) (244 mg, 1.0 equiv), tetrakis(triphenylphosphine)palladium (15.2 mg, 2.6  $\mu\text{mol}$ ), toluene (4 mL), and DMF (1 mL). The polymer yield was 53%. Anal. Calcd for  $\text{C}_{34}\text{H}_{40}\text{S}_4$ : C, 70.78; H, 6.99; S, 22.23. Found: C, 70.72; H, 7.01; S, 22.10.  $M_n = 20,000$ ,  $PDI = 2.4$ .  $T_d = 436$  °C.

**Poly{4,8-bis((2-ethylhexyl)thiophen-2-yl)-benzo[1,2-b:4,5-b']dithiophene-alt-4,8-bis(5-((2-ethylhexyl)thio)thiophen-2-yl)benzo[1,2-b:4,5-b']-dithiophene} (PBDTT-BDTT-S):** Bis(trimethyltin)4,8-bis(5-((2-ethylhexyl)thiophen-2-yl)benzo[1,2-b:4,5-b']-dithiophene (BDTT) (300 mg, 0.44 mmol) was mixed with 2,6-dibromo-4,8-bis(5-((2-ethylhexyl)thio)thiophen-2-yl)benzo[1,2-b:4,5-b']-dithiophene (2) (265 mg, 1.0 equiv), tetrakis(triphenylphosphine)palladium (15.2 mg, 2.6  $\mu\text{mol}$ ), toluene (4 mL), and DMF (1 mL). The polymer yield was 60%. Anal. Calcd for  $\text{C}_{68}\text{H}_{80}\text{S}_{10}$ : C, 67.05; H, 6.62; S, 26.33. Found: C, 66.84; H, 6.71; S, 25.89.  $M_n = 19,000$ ,  $PDI = 2.2$ .  $T_d = 410$  °C.

**Poly{4,8-bis(5-((2-ethylhexyl)thio)thiophen-2-yl)benzo[1,2-b:4,5-b']-dithiophene} (PBDTT-S):** 2,6-Bis(trimethyltin)4,8-bis(5-((2-ethylhexyl)thio)thiophen-2-yl)benzo[1,2-b:4,5-b']-dithiophene (BDTT-S) (300 mg, 0.31 mmol) was mixed with 2,6-dibromo-4,8-bis(5-((2-ethylhexyl)thio)thiophen-2-yl)benzo[1,2-b:4,5-b']-dithiophene (2) (248 mg, 1.0 equiv), tetrakis(triphenylphosphine)palladium (15.2 mg, 2.6  $\mu\text{mol}$ ), toluene (4 mL), and DMF (1 mL). The polymer yield was 51%. Anal. Calcd for  $\text{C}_{34}\text{H}_{40}\text{S}_6$ : C, 63.70; H, 6.29; S, 30.01. Found: C, 63.22; H, 6.38; S, 29.04.  $M_n = 21,000$ ,  $PDI = 2.2$ .  $T_d = 401$  °C.

#### Acknowledgements

This work was supported by National Research Foundation (NRF) grants, funded by the Korean government (NRF-2014R1A2A2A01007318 and No. 2011-0030013 through GCRC SOP). This work was also supported by the R&D Convergence Program of NST (National Research Council of Science & Technology) of Republic of Korea (CAP-15-04-KITECH).

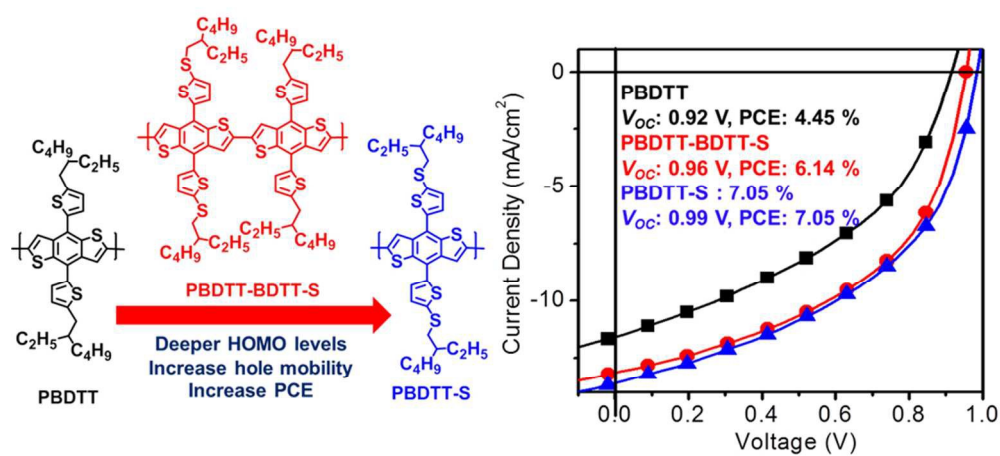
#### Notes and references

- G. Yu, J. Gao, J. C. Hummelen, F. Wudl, A. J. Heeger, *Science* 1995, **270**, 1789.
- A. J. Heeger, *Adv. Mater.* 2014, **26**, 10.
- G. Li, R. Zhu, Y. Yang, *Nat. Photonics* 2012, **6**, 153.
- J. You, L. Dou, K. Yoshimura, T. Kato, K. Ohya, T. Moriarty, K. Emery, C.-C. Chen, J. Gao, Y. Yang, *Nat. Commun.* 2013, **4**, 1446.
- Y. Liu, J. Zhao, Z. Li, C. Mu, W. Ma, H. Hu, K. Jiang, H. Lin, H. Ade, H. Yan, *Nat. Commun.* 2014, **5**, 5293.
- V. Vohra, K. Kawashima, T. Kakara, T. Koganezawa, I. Osaka, K. Takimiya, H. Murata, *Nat. Photonics* 2015, **9**, 403.
- Z. He, B. Xiao, F. Liu, H. Wu, Y. Yang, S. Xiao, C. Wang, T. P. Russell, Y. Cao, *Nat. Photonics* 2015, **9**, 174.
- C.-C. Chen, W.-H. Chang, K. Yoshimura, K. Ohya, J. You, J. Gao, Z. Hong, Y. Yang, *Adv. Mater.* 2014, **26**, 5670.
- X. Ouyang, R. Peng, L. Ai, X. Zhang, Z. Ge, *Nat. Photonics* 2015, **9**, 520.
- J.-H. Kim, J. B. Park, I. H. Jung, A. C. Grimsdale, S. C. Yoon, H. Yang, D.-H. Hwang *Energy Environ. Sci.*, 2015, **8**, 2352.
- P. M. Beaujuge, J. M. J. Fréchet, *J. Am. Chem. Soc.* 2011, **133**, 20009.
- X. Guo, C. H. Cui, M. J. Zhang, L. J. Huo, Y. Huang, J. H. Hou, Y. Li, *Energy Environ. Sci.* 2012, **5**, 7943.
- Z. B. Henson, K. Müllen, G. C. Bazan, *Nat. Chem.* 2012, **4**, 699.
- R. A. Janssen, J. Nelson, *Adv. Mater.* 2013, **25**, 1847.
- W. Ma, C. Yang, X. Gong, K. Lee, A. J. Heeger, *Adv. Funct. Mater.* 2005, **15**, 1617.
- M. T. Dang, L. Hirsch, G. Wantz, J. D. Wuest, *Chem. Rev.* 2013, **113**, 3734.
- Y. Kim, S. Cook, S. M. Tuladhar, S. A. Choulis, J. Nelson, J. R. Durrant, D. D. Bradley, M. Giles, I. McCulloch, C.-S. Ha, *Nat. Mater.* 2006, **5**, 197.
- G. Li, V. Shrotriya, J. Huang, Y. Yao, T. Moriarty, K. Emery, Y. Yang, *Nat. Mater.* 2005, **4**, 864.
- H. X. Zhou, L. Q. Yang, W. You, *Macromolecules* 2012, **45**, 607.
- T. E. Kang, T. Kim, C. Wang, S. Yoo, B. J. Kim, *Chem. Mater.*, 2015, **27**, 2653.
- D. Lee, E. Hubijar, G. J. D. Kalaw, J. P. Ferraris, *Chem. Mater.*, 2012, **24**, 2534.
- C. Cui, W.-Y. Wong, Y. Li, *Energy Environ. Sci.*, 2014, **7**, 2276.

## ARTICLE

## Journal of Materials Chemistry C

- 23 L. Ye, S. Zhang, W. Zhao, H. Yao, J. Hou, *Chem. Mater.*, 2014, **26**, 3603.
- 24 J.-H. Kim, J. B. Park, I. H. Jung, S. C. Yoon, J. Kwak, D.-H. Hwang, *J. Mater. Chem. C* 2015, **3**, 4250.
- 25 J.-H. Kim, C. E. Song, B. Kim, I.-N. Kang, W. S. Shin, D.-H. Hwang, *Chem. Mater.*, 2014, **26**, 1234.
- 26 J.-H. Kim, J. B. Park, F. Xu, D. Kim, J. Kwak, A. C. Grimsdale, D.-H. Hwang, *Energy Environ. Sci.*, 2014, **7**, 4118.
- 27 J.-H. Kim, H. S. Kim, J. B. Park, I.-N. Kang, D.-H. Hwang, *J. Polym. Sci. Part A: Polym. Chem.* 2014, **52**, 3608.
- 28 J.-H. Kim, M. Lee, H. Yang, D.-H. Hwang, *J. Mater. Chem. A*, 2014, **2**, 6348.
- 29 M. J. S. Dewar, *J. Chem. Soc.* 1950, 2329.
- 30 Y.-J. Cheng, J. Luo, S. Huang, X. Zhou, Z. Shi, T. D. Kim, D. H. Bale, S. Takahashi, A. Yick, B. M. Polishak, S.-H. Jang, L. R. Dalton, P. J. Reid, W. H. Steier and A. K.-Y. Jen, *Chem. Mater.* 2008, **20**, 5047.
- 31 C. J. Brabec, C. Winder, N. S. Sariciftci, J. C. Hummelen, A. Dhanabalan, P. A. van Hal and R. A. J. Janssen, *Adv. Funct. Mater.*, 2002, **12**, 709.
- 32 M. J. Frisch, G. W. Trucks, H. B. Schlegel, G. E. Scuseria, M. A. Robb, J. R. Cheeseman, G. Scalmani, V. Barone, B. Mennucci, G. A. Petersson, H. Nakatsuji, M. Caricato, X. Li, H. P. Hratchian, A. F. Izmaylov, J. Bloino, G. Zheng, J. L. Sonnenberg, M. Hada, M. Ehara, K. Toyota, R. Fukuda, J. Hasegawa, M. Ishida, T. Nakajima, Y. Honda, O. Kitao, H. Nakai, T. Vreven, J. A., Jr. Montgomery, J. E. Peralta, F. Ogliaro, M. Bearpark, J. J. Heyd, E. Brothers, K. N. Kudin, V. N. Staroverov, R. Kobayashi, J. Normand, K. Raghavachari, A. Rendell, J. C. Burant, S. S. Iyengar, J. Tomasi, M. Cossi, N. Rega, N. J. Millam, M. Klene, J. E. Knox, J. B. Cross, V. Bakken, C. Adamo, J. Jaramillo, R. Gomperts, R. E. Stratmann, O. Yazyev, A. J. Austin, R. Cammi, C. Pomelli, J. W. Ochterski, R. L. Martin, K. Morokuma, V. G. Zakrzewski, G. A. Voth, P. Salvador, J. J. Dannenberg, S. Dapprich, A. D. Daniels, Ö. Farkas, J. B. Foresman, J. V. Ortiz, J. Cioslowski, D. J. Fox, Gaussian, Inc., Wallingford CT, 2009.
- 33 J.-H. Kim, C. E. Song, N. Shin, H. Kang, S. Wood, I.-N. Kang, B. Kim, B. Kim, J.-S. Kim, W.-S. Shin, D.-H. Hwang, *ACS Appl. Mater. Interfaces*, 2013, **5**, 12820.
- 34 I. H. Jung, J.-H. Kim, S. Y. Nam, C. Lee, D.-H. Hwang, S. C. Yoon, *Macromolecules* 2015, **48**, 5213.



86x40mm (300 x 300 DPI)